



Effects of microporous TiO_2 support on the catalytic and structural properties of V_2O_5 /microporous TiO_2 for the selective catalytic reduction of NO by NH_3



Inhak Song^a, Seunghee Youn^a, Hwangho Lee^a, Seung Gwan Lee^b, Sung June Cho^b, Do Heui Kim^{a,*}

^a School of Chemical and Biological Engineering, Institute of Chemical Processes, Seoul National University, 1 Gwanak-ro, Gwanak-gu, Seoul 151-744, Republic of Korea

^b Department of Applied Chemical Engineering, Chonnam National University, Yongbong 300, Buk-gu, Kwangju 500-757, Republic of Korea

ARTICLE INFO

Article history:

Received 19 December 2016

Received in revised form 17 March 2017

Accepted 6 April 2017

Available online 7 April 2017

Keywords:

NH_3 -SCR

Vanadia

N_2O formation

Microporous TiO_2

ABSTRACT

Selective catalytic reduction (SCR) of NO by NH_3 over vanadium-based catalyst is often accompanied with unwanted nitrous oxide (N_2O) formation, which has 300 times higher global warming potential than CO_2 . In this work, VO_x dispersed on microporous TiO_2 catalysts calcined at various temperatures were applied to standard SCR reaction compared with VO_x on commercial TiO_2 ones. Both catalysts showed stable NO_x reduction activity although they did completely different trend in N_2O formation. Specifically, N_2O was much less produced on VO_x /microporous TiO_2 catalysts regardless of calcination temperature with or without water in the reactant. Structural characterization of the catalysts using H_2 -TPR and Vanadium XANES revealed that the microporous TiO_2 could suppress the formation of bulk-like V_2O_5 species, which are generally suggested as the main cause of N_2O formation, in comparison of non-microporous commercial TiO_2 support. Also, NH_3 -TPD and in situ DRIFTS studies showed that VO_x on microporous TiO_2 maintained strong Brønsted acidity so that it was capable of providing adsorbed NH_3 species readily up to high temperature, which led to the stable DeNOx performance. We found that such two promoting effects seemed functionally analogous to those of tungsten oxide, which is conventionally used as a promoting material for the VO_x/TiO_2 catalyst. Our results demonstrated that vanadium oxides can be effectively stabilized up to high loading by structurally modifying TiO_2 support, and also provided reasonable explanation about the promoting effects of microporous TiO_2 support on the catalytic activity and structural properties of VO_x/TiO_2 catalyst.

© 2017 Elsevier B.V. All rights reserved.

1. Introduction

More stringent regulations on NO_x emission have been implemented over the years and many DeNO_x technologies have been introduced and extensively studied in wide applications [1–6]. Selective catalytic reduction (SCR) of NO_x by ammonia is the state-of-the-art emission control technology for stationary and mobile sources. One of the commercially available catalyst is $\text{VO}_x\text{-WO}_x/\text{TiO}_2$, which is well known for its high SCR activity at 300–400 °C and strong resistance to sulfur dioxide poisoning. The ammonia SCR technology based on vanadium catalysts was successfully introduced to the power plant applications in the 1980s,

and later also applied to the heavy duty diesel vehicles by using urea solution as a portable ammonia source. Undoubtedly, vanadium based SCR catalysts will remain as a major position in the emission control area, although there are several challenging problems in real condition.

Typically, the industrial catalysts are composed of 1–2 wt.% of VO_x and about 10 wt.% of WO_x dispersed onto a titania support with anatase phase [1]. Although the amount of vanadium is a critical factor that determines NO_x reduction efficiency of SCR catalysts, its content is maintained at very low level due to its toxicity and poor stability. However, the high loading of vanadium oxides is indispensable to achieve the improved activity of the traditional vanadium based SCR catalysts especially for the low temperature performance [7]. In power plants, flue gases usually contains the high content of impurities such as alkali and alkaline salts (i.e., K, Ca), which is poisonous to the vanadium catalysts [8,9]. Such salts

* Corresponding author.

E-mail address: dohkim@snu.ac.kr (D.H. Kim).

are known to eliminate acid sites on vanadium catalyst by replacing the protons of hydroxyl groups with alkali ion which leads to severe catalyst deactivation [10,11]. Hence, increasing the amount of active vanadium site is required to prolong the lifetime of catalyst in real operating condition. In addition, for mobile combustion engine, limited available space for catalytic system requires catalysts to be highly active in a wide operating temperature range [12,13]. The vanadium concentration on the support should be maximized to overcome such space constraints. However, it is difficult to prevent the sintering of vanadium species as its loading amount increases [7]. Also, unfortunately, it has been observed that the emission of nitrous oxide (N_2O), which has higher than 300 times potential of greenhouse effect than CO_2 , also increases with the vanadia loading in the catalyst [14]. Because N_2O is a very stable compound and difficult to remove, research should be focused on the minimization of N_2O production during SCR reaction rather than its decomposition after production [3]. Therefore, it is an important technical issue to suppress the unwanted N_2O production over the vanadium SCR catalyst while maintaining the excellent NO_x reduction efficiency [15].

There has been much attention to improving the activity, selectivity, and the thermal stability of the VO_x/TiO_2 SCR catalyst by varying preparation methods and modifying TiO_2 support. Putluru et al. prepared $V_2O_5-WO_3/TiO_2$ catalysts with deposition-precipitation (DP) method instead of conventional incipient wetness impregnation, which showed the enhanced activity of catalysts prepared by the former method attributed to the change in the acidic and redox properties of vanadium species [16]. Similarly, V_2O_5/TiO_2 catalysts prepared by the equilibrium deposition filtration technique can lead to form highly dispersed vanadia on TiO_2 support, which inhibits the formation of V_2O_5 crystallites [17]. Also, mixed $TiO_2-Al_2O_3$ and TiO_2-SiO_2 materials were utilized as the support for vanadium catalysts [18–20]. According to the previous reports, mixed metal oxide supports exhibited stronger acidity, higher surface area with better thermal stability compared with pure TiO_2 support [20]. Meanwhile, a large amount of vanadium species can be incorporated into titania support by using sol-gel method [21,22]. The V_2O_5/TiO_2 catalysts prepared by sol-gel method usually had high surface area over the wide SCR active temperature range. Recently, there have been many attempts to overcome the problems of vanadium catalysts by modifying the intrinsic structural properties of the TiO_2 supports. The TiO_2 synthesized via chemical vapor condensation was used to support vanadium oxides which showed better NO_x conversion performance than catalysts prepared using commercial P25- TiO_2 [23]. Titania pillared interlayered clays (Ti-PILCs) was applied as a support for vanadia catalysts, which exhibited superior performance in SCR reaction compared with conventional V_2O_5/TiO_2 [24]. Also, Xiong et al. prepared TiO_2 nanotubes structure by using hydrothermal method, which was applied as a support for vanadium species [25]. They verified that the increase in catalytic activity was attributed to the good dispersion of V_2O_5 on TiO_2 nanotubes. Camposeco et al. similarly investigated V_2O_5 and $V_2O_5-WO_3$ on titanic acid nanotubes catalysts and found that the multi-walled morphology of nanotubes prevented the structural collapse resulting from the thermal aging up to 480 °C [26,27].

In our previous research, microporous TiO_2 with small pore less than 1 nm, which was synthesized under hydrothermal conditions in $LiOH$ solution using commercial TiO_2 anatase powder, was used as a support of vanadium oxide catalyst [28]. Vanadium oxide dispersed on microporous TiO_2 structure showed enhanced N_2 selectivity with stable NO_x reduction performance in SCR reaction in comparison of conventional catalysts. It is generally accepted that at a high vanadia coverage, surface vanadium oxide species are highly polymerized with increasing temperature because the Tamman temperature, at which solid state materials become mobile,

of vanadium oxide is near 200 °C [29]. Also, the structural properties of vanadium oxides on surface, which is highly sensitive to the calcination temperature, are closely linked to the activity and selectivity of SCR reaction [29,30]. In this work, the influence of heat treatments on the thermal stability and the structural properties of vanadium on microporous TiO_2 catalyst has been extensively investigated by using various characterization techniques compared with conventional VO_x/TiO_2 catalyst. Hence, the purpose of this study is to observe the physicochemical change of prepared catalysts as a function of calcination temperature, and also to understand the promoting effect of microporous TiO_2 on the catalytic activity and structural properties of VO_x/TiO_2 catalyst for NH_3 -SCR reaction.

2. Experimental

Microporous TiO_2 (MP- TiO_2) was synthesized by using previously reported method [28]. Briefly, 2–8 g of TiO_2 anatase (Aldrich, 98%) was added to the 10 M $LiOH$ solution in the Teflon lined autoclave for hydrothermal conversion heated at 127 °C for 72 h while stirring at 40 rpm. Then, the slurry was cooled to the room temperature and neutralized with 0.1 N HCl followed by subsequent filtration and drying. The obtained powder was used as support material after calcination under oxygen at 400 °C for 4 h. Commercial anatase TiO_2 powder (DT-51, Millennium Chemicals) was used as reference support material. For both TiO_2 supports, vanadium precursor solution was added by conventional wet impregnation method. Ammonium metavanadate (99%, Sigma Aldrich) was dissolved in 0.5 M oxalic acid solution to prepare the solution of vanadium precursor. The vanadium precursor solution containing 5 wt.% of V was mixed with TiO_2 powder and stirred for 30 min, and resulting slurry was slowly dried in a rotary evaporator. After evaporation, the obtained powder was dried overnight in an oven at 105 °C and subsequently calcined at 400, 450, 500, 550 °C for 4 h in static air condition. Catalysts were designated as the following notation VO_x /Support-Calcination temperature, for example, $VO_x/DT-51-400$ meant 5 wt.% of vanadium was loaded on TiO_2 (DT-51) and calcined at 400 °C.

N_2 adsorption–desorption of the catalysts was measured at liquid nitrogen temperature (−196 °C) by using ASAP 2010 apparatus of Micromeritics. Prior to measurement, about 0.1 g of the sample was degassed at 300 °C for more than 6 h. T-plot curves were obtained by using Harkins-Jura equation. Powder XRD patterns were taken using Ultra X18 (Rigaku) with a $Cu K\alpha$ radiation. The patterns were recorded in the range of 10–80° (2 θ) with the step size of 0.02° at the counting rate of 0.24 s per step. TG/DTA measurements were conducted in a thermal analyzer (SDT Q-600, TA Instruments) in the temperature range 25–800 °C at a heating rate of 10 °C/min in air flow (50 mL/min) on an alumina sample pan.

In situ DRIFT spectra were acquired in FT-IR spectroscopy (Nicolet 6700, Thermo Scientific) equipped with high-temperature DRIFT cell having ZnSe windows. The sample was finely ground in a porcelain mortar, and about 0.025 g of powder was rigidly packed in a circular cell to prevent the collapse of samples during heating. The IR spectra were recorded by accumulating 64 scans at a resolution of 4 cm^{-1} in all cases. For NH_3 desorption experiments, the catalyst packed in DRIFT cell was pretreated in 2% O_2 balanced with N_2 (200 mL/min) at 400 °C for 1 h to remove impurities including adsorbed water on the catalyst surface. After the pretreatment, DRIFT cell was cooled to the room temperature with N_2 purging and background spectrum was obtained in this step. Then, sample was saturated with NH_3 molecules by 500 ppm NH_3 balanced with N_2 (200 mL/min) flow at room temperature for 1 h, and subsequently purged with N_2 flow for 1 h to remove weakly adsorbed NH_3 molecules from the surface. Finally, sample was heated to

400 °C with a step of 50 °C in N₂ flow, and the temperature was held for 15 min to obtain DRIFT spectra at each temperature. The relative amount (normalized to the spectrum at 150 °C) of adsorbed NH₃ on Lewis acid site and that on Brønsted acid site was determined by comparing the maximum peak height at 1605 cm⁻¹ and 1428 cm⁻¹, respectively. For hydration experiments, KBr powder was used to obtain background spectrum at room temperature. The sample packed in DRIFT cell was pretreated in 2% O₂ balanced with N₂ (200 mL/min) at 400 °C for 1 h. De-ionized water was introduced into the flow gas by using syringe pump, and before entering the DRIFT cell, all stainless steel tubing was heated to 120 °C to prevent residual water condensation.

Hydrogen temperature-programmed reduction (H₂-TPR) profile and ammonia temperature-programmed desorption (NH₃-TPD) profile were obtained in a BEL-CAT Basic instrument (BEL Japan Inc.). About 0.05 g of prepared catalysts was loaded on quartz wool bed in a quartz U-shaped reactor. For H₂-TPR analysis, samples were pretreated at 400 °C in Ar gas at the flow rate of 50 mL/min for 1 h before measurement. After the pretreatment, samples were heated to 800 °C at the rate of 10 °C/min under 5% H₂ balanced with Ar. For TPR analysis of HNO₃-treated samples, 0.1 g of catalyst was dispersed in 200 mL of 1 M aqueous HNO₃ solution and vigorously stirred for 1 h. After washing in deionized water, the catalysts were dried and calcined at 500 °C for 1 h in static air condition. For NH₃-TPD analysis, samples were pretreated at 400 °C in He gas for 1 h and cooled to room temperature. Then, samples were exposed to 5% NH₃ balanced with He for 1 h, and subsequently pretreated at 100 °C for 1 h to remove weakly adsorbed NH₃ molecules from the surface. After the pretreatment, samples were heated to 600 °C at the rate of 10 °C/min under He flow. X-ray absorption near edge spectroscopy (XANES) around the V K-edge (E₀ = 5465 eV) were obtained in 7D beamline of the Pohang Light Source (PLS) using Si[111] monochromator. The energy scale was calibrated to a V pre-edge feature, and the intensity of X-ray was measured in a transmission mode with vanadium foil as a reference material. The obtained spectra were normalized after the correction of background using Athena software package. Inductively coupled plasma-atomic emission spectroscopy (ICP-AES) analysis were performed with OPTIMA 4300DV, Perkin-Elmer (USA).

The standard SCR activity tests were carried out in a fixed bed quartz tubular reactor, and 0.15 g of catalyst with particle size between 300 and 500 μm was used for evaluation. The reaction gas consisted of 500 ppm NO, 500 ppm NH₃, 3% H₂O (when used) and 2% O₂ balanced with N₂ and the total flow rate was 200 mL/min with the gas hourly space velocity of 80,000 mL/g h. Simulated exhaust gas was controlled by using a series of mass flow controllers connected to the gas cylinders with known composition. NO_x concentration was monitored by using NO_x chemiluminescence analyzer (42i High level, Thermo Scientific), and the concentration of N₂O was detected from FT-IR spectroscopy (Nicolet 6700, Thermo Scientific) equipped with a 2 m gas analysis cell which is heated to 120 °C. The IR spectra were recorded by accumulating 16 scans at a resolution of 1 cm⁻¹. After the reaction reached steady state, NO_x conversion was calculated based on the following equations.

$$\text{NO}_x \text{ conversion}(\%) = \frac{[\text{NO}_x]_{\text{in}} - [\text{NO}_x]_{\text{out}}}{[\text{NO}_x]_{\text{in}}} \times 100$$

3. Results

3.1. Physicochemical change of catalysts as a function of calcination temperature

Titanium oxide structure obtained by the hydrothermal conversion of commercial anatase TiO₂ in LiOH solution has several interesting features. The intercalation of Li⁺ ion into the anatase structure leads to the bond between Li⁺ ion and TiO₂ structure, and the subsequent elimination of Li⁺ ion by washing in acidic solution induces the formation of micropore on anatase surface, the size of which is estimated to be ~0.7 nm [31]. Fig. 1(a) shows the N₂ adsorption-desorption curves of two titania, MP-TiO₂ (microporous TiO₂) and commercial DT-51, and vanadium oxide supported on these two titania. DT-51 powder has similar isotherm before and after vanadium impregnation. Small hysteresis observed above the relative pressure of 0.7 may arise from the void between micrometer-sized anatase particles [32]. Meanwhile, it can be seen that MP-TiO₂ has the typical Langmuir isotherm-like curve, the characteristic of microporous structure, even after vanadium impregnation and subsequent calcination. Considering the small pore size of MP-TiO₂ and relatively large vanadium oxalate complex in impregnating solution, some small pore can be collapsed or blocked by vanadium oxide clusters during catalyst preparation. However, MP-TiO₂ and VO_x/MP-TiO₂-400 samples have quite comparable BET surface area and micropore volume with each other as shown in Table 1, indicating that vanadium is well dispersed on microporous structure of TiO₂.

Another interesting feature of MP-TiO₂ is the high crystallinity of anatase phase as shown in Fig. 1(b). It can be seen that the reflection peak at 25° arising from anatase TiO₂ (101) plane is sharper over MP-TiO₂ than DT-51. Titania with high surface area has generally low crystallinity because the thermal treatment to enhance the crystallinity of structure can also act as the driving force of structural collapse or particle aggregation [33]. In this regard, highly crystalline MP-TiO₂, which is energetically more stable than amorphous one, can be favorable for stabilizing vanadium species on surface. To confirm the thermal stability of vanadium-supported titania system, vanadium on MP-TiO₂ and DT-51 catalysts are calcined at a various temperature above 400 °C, and the results are summarized in Table 1 (Details are shown in Figs. S1 and S2). Because the vanadium oxide is thermally unstable material with the low Tamman temperature of 210 °C, calcination temperature was increased with the step of 50 °C to carefully observe the state of catalysts. It is generally accepted that vanadium oxide species can destabilize the texture of TiO₂ [1,7], and similar trend of decreasing surface area with increasing calcination temperature was found in both kinds of titania. In the case of MP-TiO₂, however, the surface area was maintained above 100 m²/g up to 500 °C, while that of DT-51 totally collapsed at 500 °C. Despite the high loading of vanadium on TiO₂, crystalline V₂O₅ was not observed up to 500 °C in both VO_x/DT-51 and VO_x/MP-TiO₂ catalysts on the basis of the XRD patterns (Fig. S2). After calcined at 550 °C, however, crystalline V₂O₅ was finally found in both samples.

In the conventional methods of loading vanadium on titania catalysts, V precursor is deposited as dissolved in oxalic acid solution [34]. This is because ammonium metavanadate can be easily dissolved in acidic solution, and also oxalate act as a capping ligand that makes a bond with vanadium ion in the solution, which is favorable for high dispersion [35,36]. In Fig. 2, TG and DTG curves are shown to investigate the decomposition and oxidation behavior of V precursor materials (vanadium oxalate) on DT-51 and MP-TiO₂ in the air condition. Small amount of water was desorbed from the surface below 200 °C, and after that, vanadium oxalate was rapidly decomposed. It can be seen that the decomposition of oxalate was finished before reaching 400 °C for both cases, which is the same as

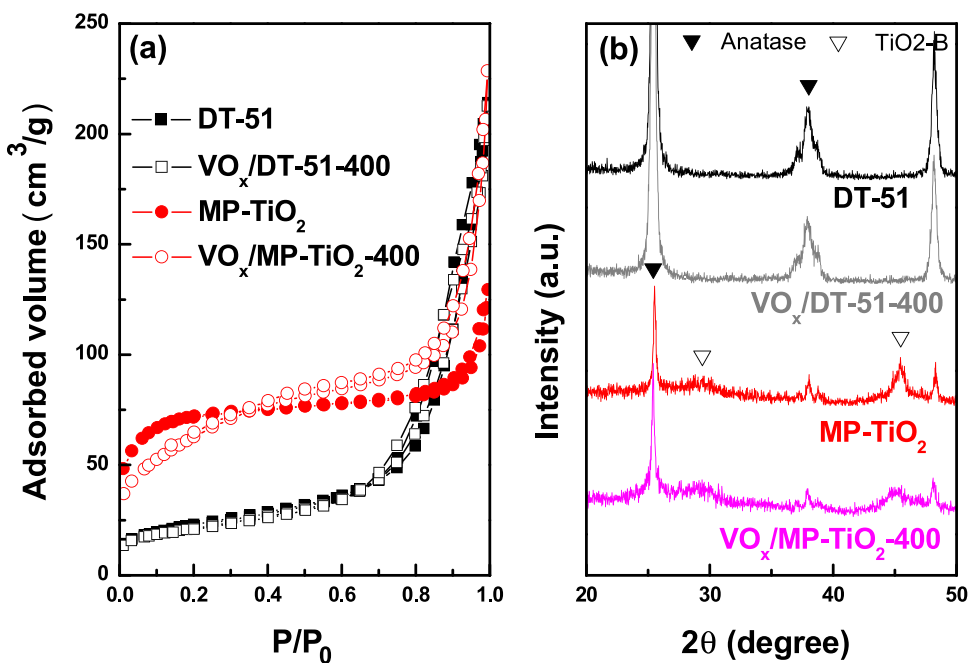


Fig. 1. (a) N_2 adsorption-desorption isotherms and (b) X-ray diffraction patterns of the samples.

Table 1

Textural properties of the TiO_2 support and the catalysts.

Catalyst	VO _x /Microporous TiO_2				VO _x /DT-51				
	V/Ti ^a (Molar ratio)	S_{BET} (m^2/g)	Crystallite size ^b (nm)	Pore volume (cm^3/g)	V/Ti ^a (Molar ratio)	S_{BET} (m^2/g)	Crystallite size ^b (nm)	Pore volume ^c (cm^3/g)	
TiO_2 support ^e	–	251	40.9	0.16	0.10	–	83	19.1	0.29
$V/TiO_2-400^{\circ}C$	0.09	230	40.1	0.26	0.09	0.11	76	19.2	0.27
$V/TiO_2-450^{\circ}C$	0.09	143	40.5	0.15	0.06	0.10	64	19.9	0.26
$V/TiO_2-500^{\circ}C$	0.09	105	37.7	0.19	0.02	0.11	14	24.1	0.04
$V/TiO_2-550^{\circ}C$	0.09	6	56.2	0.01	–	0.10	14	46.3	0.05

^a Calculated from ICP-AES results.

^b Calculated from XRD peak broadening of anatase (101).

^c Determined by single point adsorption total pore volume at a P/P_0 value of 0.97.

^d Adsorbed volume necessary to fill micropore estimated by extrapolating t-plot curve.

^e Calcined at $400^{\circ}C$ for 4 h in air condition.

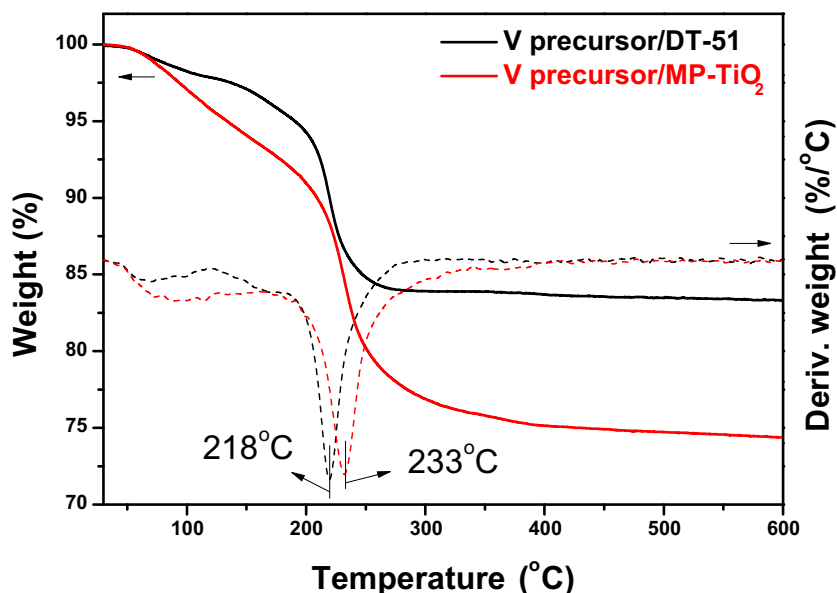


Fig. 2. Thermogravimetry and derivative thermogravimetry results of the samples under oxidative condition at a heating rate of $10^{\circ}C/min$.

previously reported result [37]. Interestingly, the peak maximum of decomposition slightly shifted to high temperature in the case of MP-TiO₂. Vanadium oxalate on DT-51 started to decompose at 200 °C and decomposition rate was maximized at 218 °C, whereas vanadium oxalate on MP-TiO₂ was not fully decomposed until 300 °C, meaning that vanadium oxalate is more stable on MP-TiO₂ than DT-51, probably due to the strong bonding between vanadium precursor and titania support. The existence of chelating material can diminish the mobility of vanadium oxide species which enhances the dispersion by preventing redistribution of vanadium active site during calcination process. Decomposition of vanadium oxalate was also shown in DTA (Differential thermal analysis) in Fig. S3. Endothermic peak near 200 °C can be undoubtedly ascribed to the same process of precursor decomposition. Likewise, endothermic peak of MP-TiO₂ is shifted to higher temperature than that of DT-51 by about 20 °C which is consistent with the TG and DTG results.

3.2. Catalytic properties of two VO_x/TiO₂ samples in SCR

VO_x supported on TiO₂ catalyst is highly active in SCR of NO with NH₃ around 300–400 °C [34]. At high temperature, however, ammonia can not only reduce NO to nitrogen but also react with oxygen to produce NO and N₂O [38]. Hence, it is generally accepted that N₂O formation from V-based catalysts is mostly attributed to the ammonia oxidation reaction, which lowers the NO conversion as temperature rises. However, N₂O formation can also occur at low temperature where 100% of NO conversion is reached because the selectivity of NO reduction with NH₃ to N₂ or N₂O strongly depends on the properties of catalysts, which is known as the nonselective catalytic reduction reaction [38]. In this section, we have focused on the selectivity of N₂O produced by reaction of NO and NH₃, not from direct NH₃ oxidation.

Fig. 3 presents the activity results of standard SCR reaction at 350 °C and 400 °C, at which catalysts are highly active, while calcination temperature of catalysts increases from 400 °C to 550 °C with the step of 50 °C. In Fig. 3(a), it can be seen that both VO_x/DT-51 and VO_x/MP-TiO₂ catalysts have remarkable NO_x reduction activity regardless of the calcination temperature, except at 550 °C, although the selectivity to N₂ is substantially different. There is almost zero emission of N₂O in VO_x/MP-TiO₂, while the amount of N₂O formation gradually increases with the calcination temperature in VO_x/DT-51. In Fig. 3(c), similar trend with the reaction at 350 °C is also found with the extremely high emissions of N₂O. In this case, interestingly, VO_x/MP-TiO₂ catalyst also shows higher selectivity to N₂ than VO_x/DT-51 catalyst. Yates et al. previously reported that the selectivity to N₂O increased with the vanadia loading in the catalyst and the SCR reaction temperature [14,39]. Based on these results, it can be assumed that the sintering or polymerization of vanadium oxide on surface, which is easily entailed with increasing vanadia loading, occurred in DT-51 but hardly happened in MP-TiO₂ support, at least up to calcination at 500 °C.

Normally, water addition in the feed is well known to strongly inhibit the N₂O formation in SCR reaction [40,41]. As shown in Fig. 3(b), humid feed fairly suppressed the N₂O emission while maintaining 100% of NO_x conversion at 350 °C for both catalysts. For the reaction at 400 °C (Fig. 3(d)), however, VO_x/DT-51 produced more than 10 ppm of N₂O even in wet condition, which similarly increased with calcination temperature. On the contrary, the amount of N₂O emitted from VO_x/MP-TiO₂ catalysts was less than 5 ppm up to 500 °C calcination. It means that the addition of water in feed can change the selectivity of NO reduction pathway from N₂O to N₂, however, it must be pointed out that N₂ selectivity is always high over MP-TiO₂ catalysts both in presence and absence of water. After the catalysts were calcined at 550 °C, N₂ selectivity was significantly decreased for both catalysts due to the

collapse of TiO₂ support as demonstrated in Table 1. Thus, it can be proposed that suppressed N₂O formation in VO_x/MP-TiO₂ catalysts may be strongly related to the structural properties of VO_x species supported on microporous TiO₂.

3.3. Characterization of the vanadium oxide structure

Dispersed vanadium oxide species on TiO₂ have clearly different structure and properties from that of bulk oxide, which leads to different catalytic activity and selectivity in NH₃-SCR reaction [1,29]. Especially, polymerization or sintering process of dispersed VO_x species on TiO₂ surface is a main reason for the increase in the selectivity to N₂O in SCR reaction according to the literature [7,14]. In Fig. 4(a) and (b), H₂-TPR profiles of VO_x/DT-51 and VO_x/MP-TiO₂ catalysts calcined at various temperatures (400, 450, 500, 550 °C) are compared with those of the bare TiO₂ supports. The reduction behavior of the dispersed VO_x on TiO₂ was extensively studied in literature [42–45]. In general, V⁵⁺ species are reduced to V³⁺ without further reduction which occurs by the elimination of the terminal oxygen atoms of the V=O groups. This is reasoned by the fact that the oxygen atoms of V=O groups are more labile than those of the polymerized V—O—V groups [30]. Both MP-TiO₂ and DT-51 supports demonstrated the H₂ reduction peak between 500 and 600 °C arising from the elimination of reducible oxygen on TiO₂ surface [46]. DT-51 showed much bigger reduction peak near 580 °C, due to the reduction of the sulfate species to SO₂ that DT-51 contained initially [32]. For the case of VO_x/DT-51 catalysts, dispersed vanadium oxides are mainly reduced between 400 and 600 °C in almost one step. Interestingly, the reduction peak position is shifted to higher temperatures as the calcination temperature of catalysts increases while the amount of consumed H₂ remains almost unchanged. Reducibility of vanadium species is correlated with the vanadium oxide structure based on the previous report that with the increasing degree of polymerization, the reduction peak should shift to higher temperatures [42,44]. Thus, it can be suggested that the peak shift of VO_x/DT-51 samples is attributed to the growth of bulk-like V₂O₅ domain, which is consistent with the results described above. In the case of VO_x/MP-TiO₂ samples, however, the peak position around at 487 °C was not changed up to the calcination temperature of 500 °C, which apparently suggests that the growth of large VO_x particles that are reduced by H₂ at high temperature is suppressed on MP-TiO₂ compared to DT-51 support. When the calcination temperature of VO_x/MP-TiO₂ was increased to 550 °C, the reduction peak was shifted to 537 °C as expected based on the results above. To investigate in more detail, TPR profiles of both catalysts calcined at 500 °C before and after the HNO₃ treatment are shown in Fig. 4(c) and (d). HNO₃ treatment is expected to remove polymerized VO_x including bulk-like V₂O₅ species from TiO₂ surface, while monomeric vanadium species are chemically stable due to strong interaction with TiO₂ support [44]. As expected, reduction peak after HNO₃ washing is shifted to lower temperature of 470 °C in VO_x/DT-51-500 catalyst and 468 °C in VO_x/MP-TiO₂-500 catalyst, which is attributed to the reduction of monomeric VO_x species. Such observation demonstrates that the peak shift of vanadium reduction is mainly due to the polymerization of VO_x species. Also, hydrogen consumption during H₂ TPR of VO_x/DT-51 and VO_x/MP-TiO₂ after HNO₃ washing was 34% and 65% of fresh ones, respectively, which means that vanadium oxides on DT-51 were more severely polymerized than those on MP-TiO₂. The amount of leached vanadium during the HNO₃ treatment calculated by ICP-AES results (not shown) was 64% for VO_x/DT-51 and 42% for VO_x/MP-TiO₂, respectively. In the meantime, it can be seen that there is a small shoulder peak at 538 °C in VO_x/MP-TiO₂. Even though the catalysts were washed in large batch for a sufficient time, such high temperature reduction signal remained, which can be attributed to the existence of residual bulk-like V₂O₅ that can-

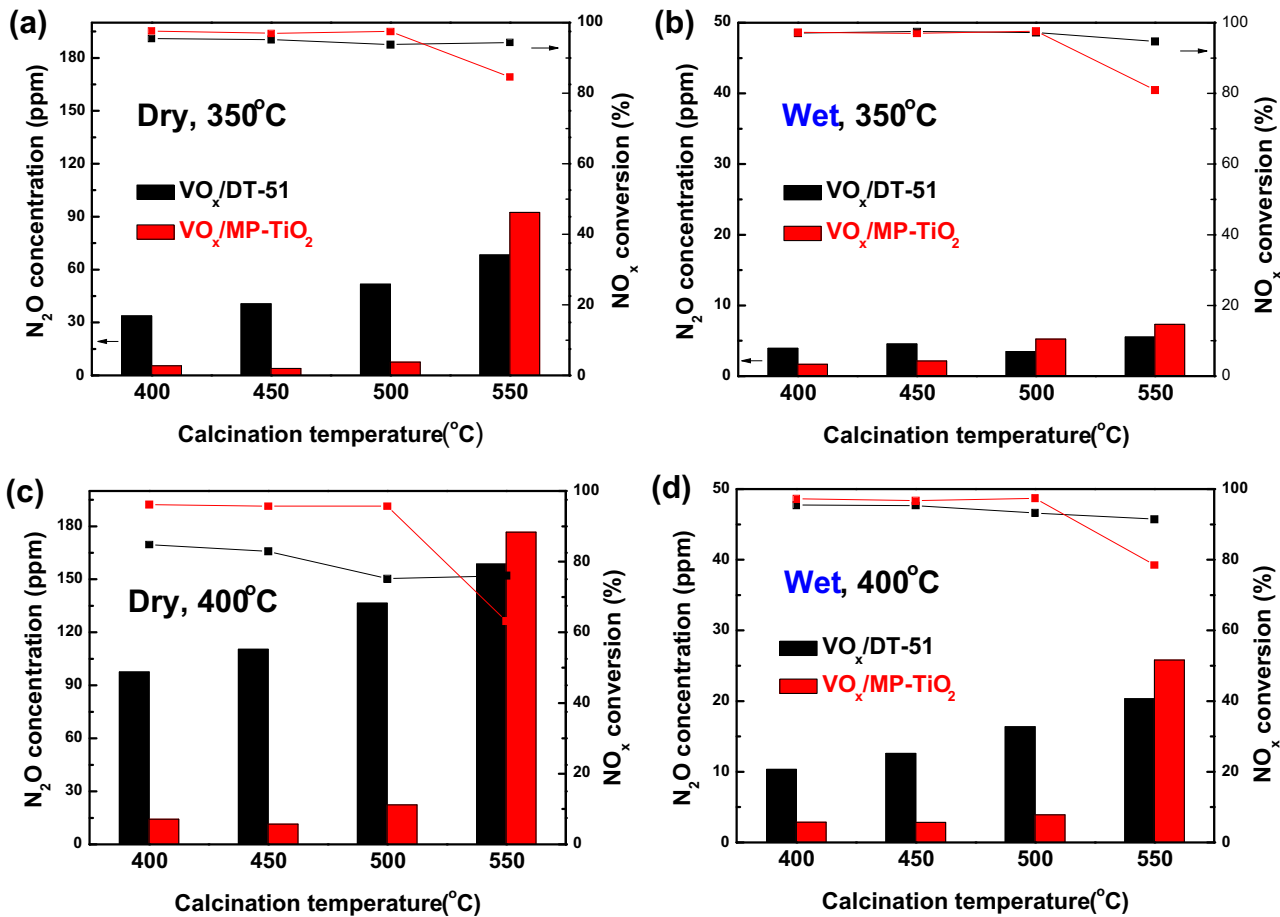


Fig. 3. NO_x conversion and N_2O concentration during SCR of NO with NH_3 over the $\text{VO}_x/\text{DT-51}$ and $\text{VO}_x/\text{MP-TiO}_2$ catalysts calcined at a various temperature. Measurement was performed after reaching steady state in (a) dry condition at 350°C , (b) wet condition at 350°C , (c) dry condition at 400°C , and (d) wet condition at 400°C .

not be accessible in acidic solution. Presumably, these species were confined inside TiO_2 structure during the collapse of microporous structure as evidenced in Table 1, and also hardly accessible by gas phase molecules during the reaction, which may hinder the undesirable participation of bulk-like V_2O_5 in SCR reaction.

The change of the vanadium oxides supported on DT-51 and MP-TiO₂ upon increasing calcination temperature was also investigated by vanadium X-ray absorption near-edge spectroscopy (XANES) to understand the local environment of VO_x compound. The normalized vanadium K-edge XANES spectra are shown in Fig. 5(a) for $\text{VO}_x/\text{DT-51}$ and Fig. 5(b) for $\text{VO}_x/\text{MP-TiO}_2$ catalysts, respectively, in addition to the reference materials. It is confirmed that vanadium deposited on both TiO_2 , just dried sample before calcination, existed in exactly same structure of vanadium oxalate (Fig. S4). Because vanadium atoms are coordinated with oxalate, it is reasonable that the valence of the vanadium species on TiO_2 is close to 4 before calcination step [36] which is evidenced by the main edge position (Fig. S5). Interestingly, after the decomposition of oxalate by calcination, the shape of the post-edge of $\text{VO}_x/\text{DT-51}$ and $\text{VO}_x/\text{MP-TiO}_2$ evolved with noticeably different pattern although the valence of vanadium was maintained as 5 on both samples. In the case of $\text{VO}_x/\text{DT-51}$, the characteristics of post-edge were quite different from ammonium metavanadate (NH_4VO_3), which is precursor material, and became similar to the post-edge of V_2O_5 with increasing temperature. On the contrary, the post-edge of $\text{VO}_x/\text{MP-TiO}_2$ obviously resembled that of NH_4VO_3 , which reflects the similar coordination geometry of dispersed VO_x on MP-TiO₂ to that of $[\text{VO}_3]^-$ species. Metavanadate adopts a polymeric structure consisting of linear chains of $[\text{VO}_3]^-$ that formed by

corner-sharing VO_4 tetrahedra unit [47]. Hence, it can be suggested that VO_x species on MP-TiO₂ will be polymerized to the linearly connected oligomeric species in confined space, without polymerizing randomly into bulk-like VO_x particles at least up to 450°C . After the collapse of microporous structure at 550°C , however, V_2O_5 -like post-edge appeared in $\text{VO}_x/\text{MP-TiO}_2$. Thus, such observation suggests a reasonable explanation about how the formation of bulk-like V_2O_5 species can be suppressed on the microporous TiO_2 support.

3.4. Acid properties of the catalysts

It has long been known that NH_3 -SCR activity and selectivity is closely correlated with the acidity of catalysts, because reaction readily occurs in Eley-Rideal mechanism by which NH_3 participate in the reaction as adsorbed on the surface [1,48]. To investigate the acidic properties of the catalysts, NH_3 -TPD (Temperature-programmed desorption) curves of $\text{VO}_x/\text{DT-51}$ and $\text{VO}_x/\text{MP-TiO}_2$ calcined at 400°C are compared as shown in Fig. 6(a). It can be seen that the majority of acid sites are observed in the temperature range from 150 to 350°C for both catalysts. In this region, the amount of desorbed ammonia is slightly higher over $\text{VO}_x/\text{MP-TiO}_2$ than $\text{VO}_x/\text{DT-51}$ catalyst, which indicates that the former sample possesses the higher number of relatively weak acid sites. A major difference lies in the strong acid site, which desorbs NH_3 at 427°C over $\text{VO}_x/\text{MP-TiO}_2$, although $\text{VO}_x/\text{DT-51}$ does not have, as evidenced by the complete desorption below 400°C . Meanwhile, the desorption curve of $\text{VO}_x/\text{MP-TiO}_2-400$ sample was not dropped to the background level until 500°C due to low calcina-

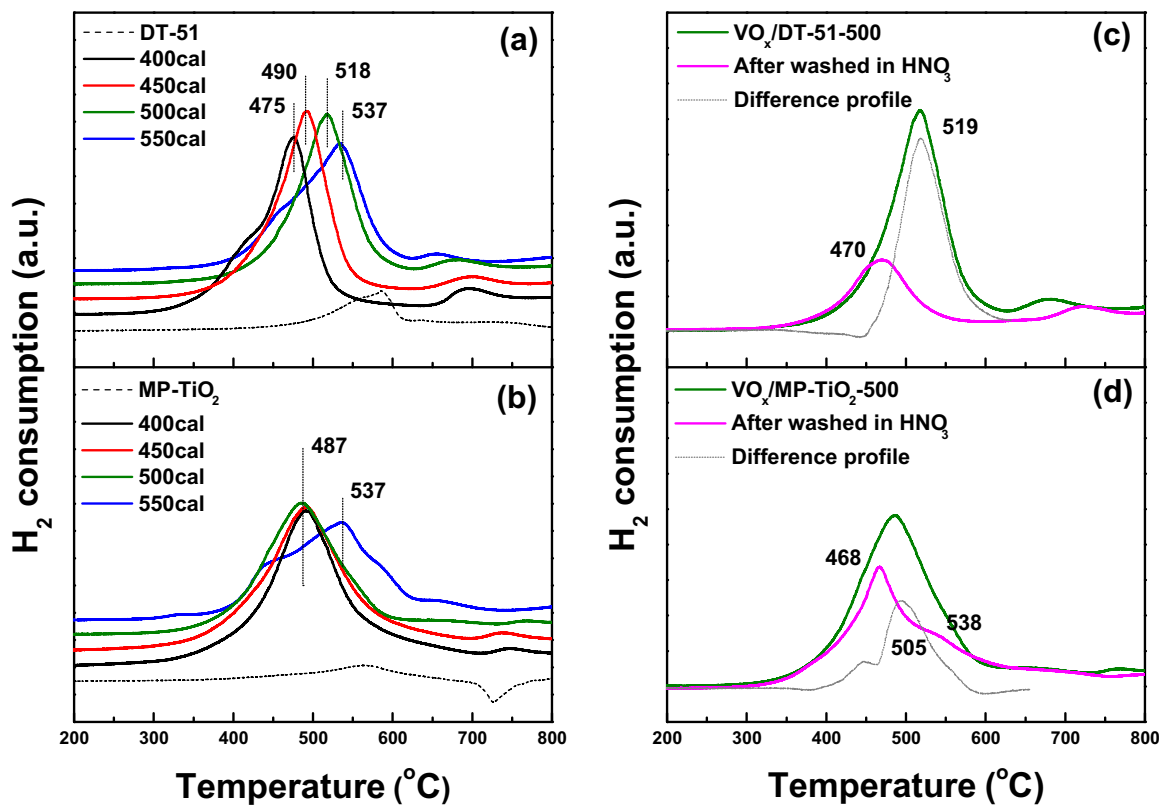


Fig. 4. H_2 -TPR spectra of (a) $\text{VO}_x/\text{DT-51}$ and (b) $\text{VO}_x/\text{MP-TiO}_2$ catalysts calcined at a various temperature. In addition, TPR profile of $\text{VO}_x/\text{DT-51-500}$ and $\text{VO}_x/\text{MP-TiO}_2-500$ catalysts before and after treatment in HNO_3 was shown in (c,d).

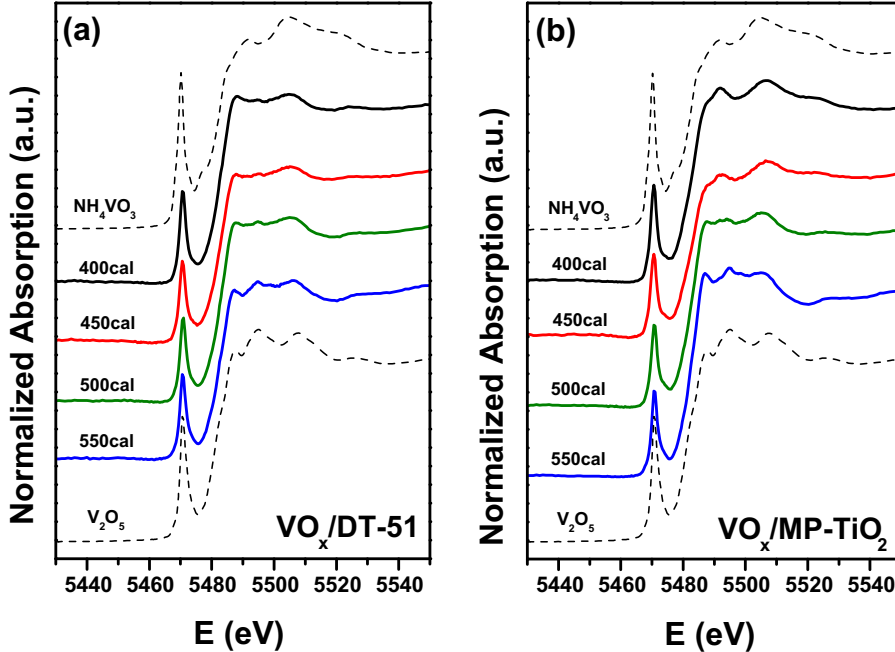


Fig. 5. Normalized V K-edge XANES spectra of (a) $\text{VO}_x/\text{DT-51}$ and (b) $\text{VO}_x/\text{MP-TiO}_2$ catalysts calcined at a various temperature as well as reference materials.

tion temperature, which makes it difficult to directly compare the acid amount of both catalysts. Therefore, TPD curves of $\text{VO}_x/\text{DT-51}$ and $\text{VO}_x/\text{MP-TiO}_2$ catalysts calcined at 500°C are compared in Fig. 6(b). In this case, there is more remarkable difference between two samples. The amount of desorbed NH_3 of two samples is quite similar in the temperature range from 150 to 300°C , however,

it is evident that stronger acid site centered at 400°C exist on $\text{VO}_x/\text{MP-TiO}_2$ catalyst. It is noteworthy that the amount of acid site declined for both type of catalysts as the calcination temperature increased, while the strong acid sites near 400°C were retained in $\text{VO}_x/\text{MP-TiO}_2$ catalyst. To understand the origin of strong acid sites on $\text{VO}_x/\text{MP-TiO}_2$ catalyst, *in situ* DRIFT spectra during temper-

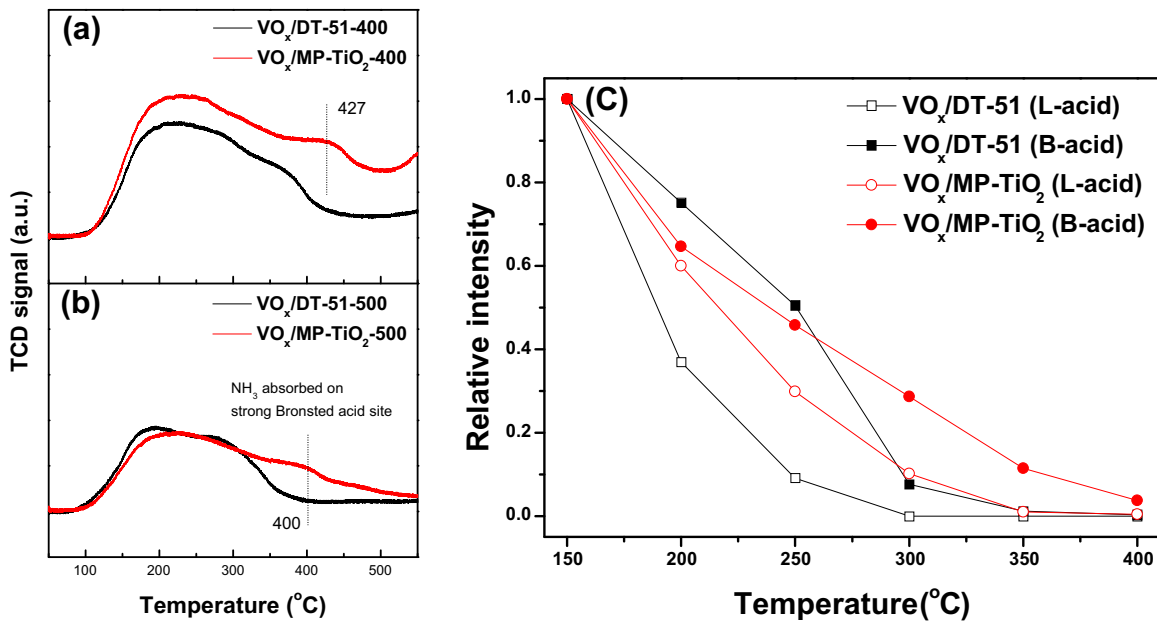


Fig. 6. NH₃-TPD curves of the VO_x/DT-51 and VO_x/MP-TiO₂ catalysts calcined at (a) 400 °C and (b) 500 °C. (c) The relative amount (normalized to initial spectrum at 150 °C) of Bronsted acid sites (open symbol) and Lewis acid sites (closed symbol) of VO_x/DT-51-500 and VO_x/MP-TiO₂-500 catalyst determined from FT-IR of adsorbed NH₃ at 1428 cm⁻¹ and 1605 cm⁻¹ as a function of temperature.

ature ramping was acquired after saturating the catalyst surface with chemisorbed NH₃ as shown in Fig. S6. After NH₃ adsorption and subsequent purging with N₂, a strong band at 1428 cm⁻¹ appeared which is assigned to the ionic ammonium on Brønsted acid sites [49,50]. Also, a band at 1605 cm⁻¹ came out which is related to the coordinated ammonia on Lewis acid sites [49,50]. Thereafter, the relative amount of adsorbed NH₃ on each site was determined as a function of temperature by measuring the intensity of peak. Fig. 6(c) summarizes the change in the relative intensity of adsorbed NH₃ on Lewis and Brønsted acid sites as a function of temperature, respectively, which directly compares the strength of acid sites on VO_x/DT-51 and VO_x/MP-TiO₂ catalysts. In our experiment, both catalysts lose Lewis-adsorbed NH₃ more rapidly than Brønsted-adsorbed NH₃ with increasing temperature. Such fact indicates that although TiO₂ support is mostly Lewis acidic material, high coverage of VO_x species on that surface leads to the generation of abundant strong Brønsted acid sites on VO_x/TiO₂ catalysts [50,51]. The amount of Brønsted acid sites on VO_x/DT-51 declines more rapidly as the temperature increases to 300 °C. VO_x/MP-TiO₂ catalyst, however, retains some Brønsted-adsorbed NH₃ at high temperature. More than 10% of Brønsted-adsorbed NH₃ survives even at 350 °C. This means that VO_x species supported on MP-TiO₂ have slightly stronger Brønsted acid site than VO_x/DT-51 catalyst, which is well matched with NH₃-TPD results above. The role of the strong acid sites on NO reduction reaction will be discussed later in terms of the selectivity to N₂O.

4. Discussion

4.1. Inhibition of bulk-like V₂O₅ formation in microporous TiO₂

According to the current study about vanadium oxides loaded on the two kinds of TiO₂ support, commercial DT-51 and microporous TiO₂, it was found that the selectivity to N₂O was significantly suppressed in VO_x on the latter support. It has been known that there is an intimate relationship between the structure of dispersed VO_x species, and catalytic activity and selectivity in NH₃-SCR reaction. At low vanadia loadings, VO_x species mainly exists as monomeric or polymeric vanadate species. As the loading of vanadia increased,

bulk-like V₂O₅ particles can be formed at the expense of the polymeric vanadate species [29,30]. Also, such polymerization can be accelerated by thermal aging, which leads to a weak thermal stability of catalyst with high vanadia loading [7,12]. However, catalyst with low vanadia loading is not sufficient because monomeric vanadate is less active in SCR reaction in spite of their excellent selectivity for N₂ formation. It is generally accepted that polymeric vanadate species are highly active in SCR reaction compared to monomeric species [29,45]. According to the reaction scheme suggested by Topsøe et al., at least two neighboring V atoms are required in the SCR reaction to combine an acid cycle with redox cycle that accounts for the high activity of polymeric VO_x species [4,52]. However, the formation of bulk-like V₂O₅ is suggested as the main reason for catalyst deactivation. Thus, controlling the degree of VO_x polymerization on TiO₂ support to maximize the density of polymeric vanadate without forming the bulk-like V₂O₅ is essential to elicit a best performance from vanadia catalysts in SCR reaction. For the case of VO_x/DT-51 catalyst, the amount of produced N₂O was correlated to that of bulk-like V₂O₅ species as shown in Fig. 3 even in the condition of almost 100% NO_x conversion. However, VO_x/MP-TiO₂ catalyst on which the formation of bulk-like V₂O₅ was suppressed showed almost no emission of N₂O at least up to 500 °C. Therefore, it can be concluded that N₂O in SCR reaction was produced less by inhibiting the formation of large size V₂O₅ on microporous TiO₂ support.

Meanwhile, there is a large difference in initial surface area of both TiO₂ supports, so that the surface density of vanadate species is quite different over VO_x/DT-51 and VO_x/MP-TiO₂ catalysts. Considering that the surface density of VO_x is an important factor that determines the degree of polymerization of VO_x species on the surface [53,54], we have to compare the samples with similar vanadium surface density. Fortunately, VO_x/DT-51-400 catalyst and VO_x/MP-TiO₂-500 catalyst had similar vanadium surface density of 7.6 V/nm² and 7.1 V/nm², respectively, which are below theoretical monolayer coverage [21]. These values were calculated based on ICP-AES results (not shown). As shown in Fig. 3, the amount of N₂O produced in dry condition at 400 °C was 98 ppm over the former, however, 22 ppm over the latter. Also, in the wet condition, VO_x/DT-51-400 produced 11 ppm of N₂O, while VO_x/MP-TiO₂-500

did only 4 ppm. Therefore, with the similar surface concentration of vanadium oxides on surface, microporous TiO_2 can suppress the formation of bulk-like V_2O_5 which leads to high selectivity for N_2 formation.

In addition, to confirm the effect of microporous structure more clearly, we have prepared titania nanotube as reference support material. Titania nanotube was easily obtained by the hydrothermal conversion of commercial anatase TiO_2 using NaOH solution instead of LiOH as previously reported method [31]. BET surface area of nanotube structure was $235 \text{ m}^2/\text{g}$ after calcination at 400°C , which is fairly comparable to that of microporous TiO_2 (Fig. S7). However, average pore size of nanotube structure was 10.7 nm, while that of microporous TiO_2 was only 2.6 nm, which means that nanotube structure contains a large amount of mesopore as shown in Fig. S7. Therefore, the effect of microporosity on VO_x polymerization can be separated from that of high surface area by comparing vanadium catalysts supported on these two different supports. As shown in Fig. 7, the emission of N_2O was significantly suppressed on microporous TiO_2 compared to nanotube structure as well as DT-51 in the temperature range of $350\text{--}450^\circ\text{C}$, even with relatively stable SCR performance at high temperature. Thus, it can be concluded that microporous TiO_2 play a critical role in inhibiting the formation of bulk-like V_2O_5 , which prevents nonselective catalytic reduction route and ammonia oxidation.

4.2. Effect of surface hydration at operating temperature on N_2O formation

One of the interesting features of the selectivity in SCR reaction is that water in feed gas can effectively prevent the formation of N_2O [41]. Topsøe et al. proposed that the intermediate of SCR reaction and N_2O formation is same [40]. They suggested a nitrosamidic species (NH_xNO) as an intermediate which could be decomposed to N_2O in dry condition, while it could be also decomposed to N_2 in the presence of water. In addition, they found that the surface hydroxylated with water leads to more Brønsted acid sites, which could interact with adsorbed ammonia. In our experiment, the presence of water sufficiently prevented N_2O formation for both catalysts, while still much higher amount of N_2O was produced in $\text{VO}_x/\text{DT-51}$ than $\text{VO}_x/\text{MP-TiO}_2$ catalyst. According to the assumption of Topsøe et al., water molecules should stay in contact with surface to affect the decomposition of intermediate [40], and we have tried to focus on the degree of surface hydration of catalysts at SCR operating temperature. In Fig. 8, the surface of (a) $\text{VO}_x/\text{DT-51-400}$ and (b) $\text{VO}_x/\text{MP-TiO}_2-400$ at 400°C was observed by *in situ* DRIFT in the presence or absence of water. The broad band at about $3200\text{--}3400 \text{ cm}^{-1}$ can be assigned to OH stretching of the adsorbed water molecules which are hydrogen bonded to the surface of catalysts [55]. As temperature increases, the intensity of the bands gradually decreases due to the desorption of water molecules from the surface and it can be seen that a small amount of water still exists on both catalysts at 400°C even in dry condition. It is noteworthy that the V-OH hydroxyl groups at 3650 cm^{-1} are found in only $\text{VO}_x/\text{MP-TiO}_2$ catalyst which indicates that the catalyst can still provide Brønsted acid site at 400°C . However, it is shown that $\text{VO}_x/\text{DT-51}$ catalyst cannot provide any Brønsted acid site even in the presence of water at such high temperature. When water is fed into the catalysts, there is a definite difference in surface hydration between $\text{VO}_x/\text{DT-51}$ and $\text{VO}_x/\text{MP-TiO}_2$ sample. The relative amount of adsorbed H_2O on the surface of both catalysts were normalized and compared as shown in Fig. 8(c). In the case of $\text{VO}_x/\text{DT-51}$ catalyst, the intensity of adsorbed water molecules increased by about 2.5 times in wet stream. However, for the $\text{VO}_x/\text{MP-TiO}_2$ catalyst, the intensity of adsorbed water molecules increased by about 4 times in wet stream and Brønsted acidity also increased in the presence of water which is consistent with the observation of other results.

Similar trends was found in the same experiment at 350°C . Such observations propose that $\text{VO}_x/\text{MP-TiO}_2$ catalyst can more easily stabilize adsorbed water molecules compared to $\text{VO}_x/\text{DT-51}$ catalyst in wet condition. Thus, it can be suggested that an intermediate is more likely to decompose to N_2 rather than N_2O on hydrated $\text{VO}_x/\text{MP-TiO}_2$ surface compared with $\text{VO}_x/\text{DT-51}$ in the presence of water, which can explain why much higher amount of N_2O was still produced over $\text{VO}_x/\text{DT-51}$ than $\text{VO}_x/\text{MP-TiO}_2$ catalyst even in the presence of water.

4.3. Analogy of microporosity in TiO_2 to W promotor

According to our results, vanadium oxides on microporous TiO_2 had a larger amount of acid sites, especially strong Brønsted acid site, than those on DT-51 support. A further question arises about how the amount and strength of acid site can affect the catalytic performance in SCR reaction. It has been known that VO_x/TiO_2 catalyst can be normally promoted by WO_x species in NO reduction reaction [1,56]. The operating window of W-promoted vanadium catalysts becomes much larger than vanadium-only catalyst, which means that NO_x conversion is maintained as more than 90% up to relatively high temperature region. Many authors reported that the acidity of vanadium catalysts is largely increased in the presence of W, and these acid sites are able to adsorb NH_3 molecules on catalyst surface up to high temperature [57,58]. Adsorbed NH_3 can migrate to active site on surface and participate in SCR reaction with gaseous NO [59], and thus, undesired NH_3 oxidation with O_2 can be suppressed with increased acidity. Likewise, it can be proposed that the strong acid sites on $\text{VO}_x/\text{MP-TiO}_2$ catalyst readily provide stable adsorbed NH_3 species that can react with NO rather than O_2 , which enhances the stability of SCR reaction. Also, WO_x was reported to prevent the formation of crystalline V_2O_5 during catalyst aging [60]. Recently, several groups have reported about the roles of tungsten oxides on vanadium catalysts. Kompio et al. found that the promotional effect of WO_x stems from the inhibition of island formation of the surface vanadium oxide species [54]. Vanadium island, here, represents the large polymeric vanadate which are produced at the expense of small polymeric vanadate with low nuclearity such as dimer or trimer. They attributed superior activity over W containing catalyst to the formation of small vanadate with low nuclearity rather than large vanadium island. It is noteworthy that the similar effect is also found in our vanadium catalyst supported on microporous TiO_2 . In spite of the high loading of vanadium oxides, VO_x species are separately dispersed in confined micropore, which leads to the inhibition of bulk-like large vanadium clustering up to 500°C . Thus, polymerization of vanadium can be optimized to maximize the density of the small vanadate with low nuclearity rather than the large vanadium clusters in microporous TiO_2 . It is interestingly pointed out that there is a functional analogy between W-promoted vanadium catalyst and microporous TiO_2 -supported vanadium catalyst. Modifying titania structure gave rise to two primary changes in the properties and structure of vanadium species on surface, the inhibition of bulk-like V_2O_5 formation and the existence of strong Brønsted acidity, which are similar to the promoting effect of tungsten oxides as mentioned above. Also, such changes led to the thermally stable catalyst even at high V loading, resulting in suppressed N_2O formation in SCR reaction. Meanwhile, the promotional effects disappeared after the collapse of microporous structure with calcination at 550°C , which might be due to the high loading of vanadium. Therefore, enhancing the stability of microporous TiO_2 support up to high temperature is strongly required for further applications.

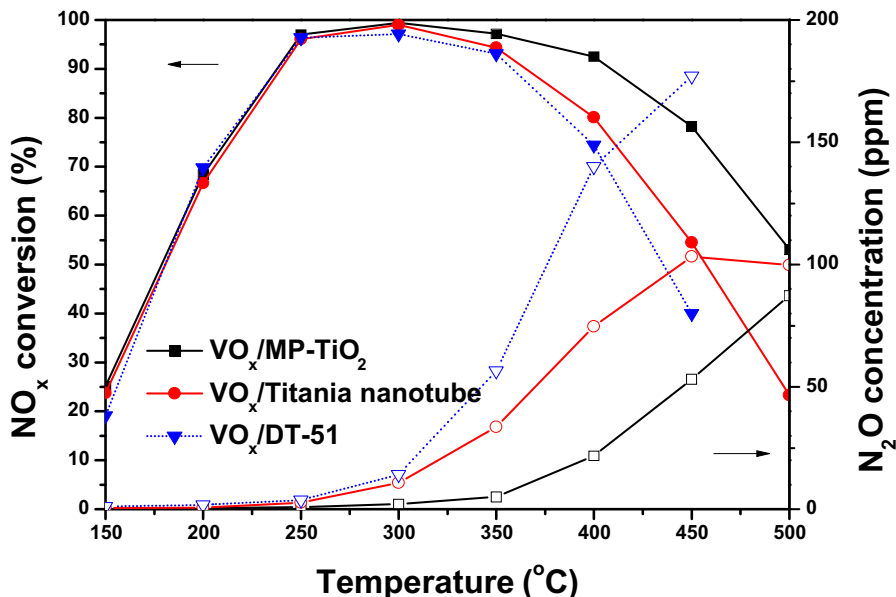


Fig. 7. NO_x conversion and N₂O concentration during the standard SCR over the VO_x/Microporous TiO₂, VO_x/Titania nanotube and VO_x/DT-51 catalysts calcined at 500 °C (GHSV = 80,000 mL g⁻¹ h⁻¹, Inlet: 500 ppm NO, 500 ppm NH₃, 2% O₂, and balanced with N₂).

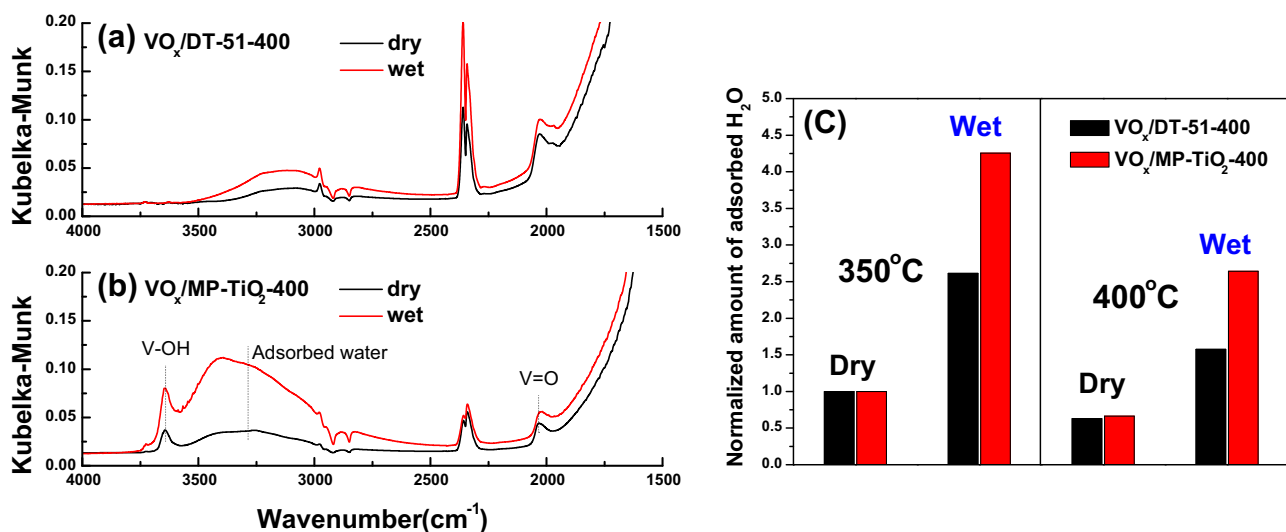


Fig. 8. In situ DRIFT spectra of (a) VO_x/DT-51-400 and (b) VO_x/MP-TiO₂-400 catalysts at 400 °C under dry (N₂) and wet condition (3% H₂O was fed into the purge gas). The relative amount (normalized to the spectrum at 350 °C with dry condition) of adsorbed H₂O on the surface of VO_x/DT-51-500 and VO_x/MP-TiO₂-500 catalyst in dry and wet condition determined from DRIFT spectra by comparing the maximum peak height between 2800 cm⁻¹ and 3600 cm⁻¹.

5. Conclusions

In the selective catalytic reduction over vanadium-based catalysts, the amount of vanadium should be increased to obtain low temperature performance, leading to accompany the unwanted production of N₂O which has considerable greenhouse gas potential. In this work, 5 wt.% V on microporous TiO₂ and 5 wt.% V on commercial TiO₂ (DT-51) catalysts calcined at 400, 450, 500, and 550 °C were applied in standard SCR reaction at temperature of 350 and 400 °C. In the case of VO_x/commercial TiO₂ (DT-51), the production of N₂O gradually increased with the calcination temperature, which was attributed to the formation of bulk-like V₂O₅ species. In contrast, it was observed that the yield of N₂O was significantly suppressed on VO_x/microporous TiO₂ catalysts up to the calcination temperature of 500 °C with or without water on gas stream, while maintaining stable NO_x reduction efficiency. Based

on the comparative physicochemical characterization for the two different catalysts, it was confirmed that the growth of large VO_x particles, which is the main reason of N₂O production, was inhibited in microporous TiO₂ while retaining the structure of linearly connected metavanadate chains dominantly at least up to 450 °C. It was also found that the amount of acid sites declined over both catalysts as the calcination temperature increased, while strong Brønsted acid sites still remained more abundantly in VO_x/microporous TiO₂ catalyst, which is beneficial to maintain the stable performance in high temperature SCR reaction. Furthermore, we confirmed that VO_x/microporous TiO₂ catalyst exhibited excellent selectivity to N₂ even compared with VO_x/non-microporous TiO₂ nanotube, which demonstrated the effect of microporosity in suppressing N₂O production. In conclusion, VO_x dispersed on microporous TiO₂ was proved to be a thermally stable catalyst up to 500 °C at high V load-

ing with suppressed N₂O formation and high DeNOx activity in SCR reaction.

Acknowledgments

This research was supported by the R&D Center for reduction of Non-CO₂ Greenhouse gases (0458-20160034) funded by Korea Ministry of Environment (MOE) as Global Top Environment R&D Program. X-ray absorption near edge structure (XANES) experiment was conducted at the 7D beamline of the Pohang Accelerator Laboratory (PAL). The authors acknowledge the World Class 300 Project Programs (0458-20160057) funded by the Korea Institute for Advancement of Technology (KIAT) for the financial support.

Appendix A. Supplementary data

Supplementary data associated with this article can be found, in the online version, at <http://dx.doi.org/10.1016/j.apcatb.2017.04.016>.

References

- [1] G. Busca, L. Lietti, G. Ramis, F. Berti, *Appl. Catal. B* 18 (1998) 1–36.
- [2] M. Fu, C. Li, P. Lu, L. Qu, M. Zhang, Y. Zhou, M. Yu, Y. Fang, *Catal. Sci. Technol.* 4 (2014) 14–25.
- [3] B. Guan, R. Zhan, H. Lin, Z. Huang, *Appl. Therm. Eng.* 66 (2014) 395–414.
- [4] N.-Y. Topsoe, *Science* 265 (1994) 1217–1219.
- [5] X. Wang, W. Wu, Z. Chen, R. Wang, *Sci. Rep.* 5 (2015) 9766.
- [6] I. Song, S. Youn, D.H. Kim, *Top. Catal.* 59 (2016) 1008–1012.
- [7] G. Madia, E. Koebel, M.F. Raimondi, A. Wokaun, *Appl. Catal. B* 39 (2002) 181–190.
- [8] L. Chen, J. Li, M. Ge, *Chem. Eng. J.* 170 (2011) 531–537.
- [9] R. Khodayari, C.U.I. Odendbrand, *Appl. Catal. B* 30 (2001) 87–99.
- [10] O. Kröcher, M. Elsener, *Appl. Catal. B* 77 (2008) 215–227.
- [11] D. Nicosia, I. Czekaj, O. Kröcher, *Appl. Catal. B* 77 (2008) 228–236.
- [12] A. Marberger, M. Elsener, D. Ferri, O. Kröcher, *Catalysts* 5 (2015) 1704–1720.
- [13] A. Marberger, M. Elsener, D. Ferri, A. Sagar, K. Schermanz, O. Kröcher, *ACS Catal.* 5 (2015) 4180–4188.
- [14] J.A. Martín, M. Yates, P. Ávila, S. Suárez, J. Blanco, *Appl. Catal. B* 70 (2007) 330–334.
- [15] T.J. Wallington, P. Wiesen, *Atmos. Environ.* 94 (2014) 258–263.
- [16] S.S.R. Putluru, L. Schill, D. Gardini, S. Mossin, J.B. Wagner, A.D. Jensen, R. Fehrmann, *J. Mater. Sci.* 49 (2014) 2705–2713.
- [17] I. Georgiadou, C. Papadopoulou, H.K. Matralis, G.A. Voyatzis, A. Lycourghiotis, C. Kordulis, *J. Phys. Chem. B* 102 (1998) 8459–8468.
- [18] G. Clarebout, M. Ruwet, H. Matralis, P. Grange, *Appl. Catal.* 76 (1991) L9–L14.
- [19] B.M. Reddy, S. Mehdi, E.P. Reddy, *Catal. Lett.* 20 (1993) 317–327.
- [20] M. Kobayashi, R. Kuma, S. Masaki, N. Sugishima, *Appl. Catal. B* 60 (2005) 173–179.
- [21] S.B. Kristensen, A.J. Kunov-Kruse, A. Riisager, S.B. Rasmussen, R. Fehrmann, *J. Catal.* 284 (2011) 60–67.
- [22] X. Zhang, X. Li, J. Wu, R. Yang, Z. Zhang, *Catal. Lett.* 130 (2009) 235–238.
- [23] W. Cha, S. Chin, E. Park, S.-T. Yun, J. Jurng, *Appl. Catal. B* 140–141 (2013) 708–715.
- [24] H.J. Chae, I.-S. Nam, S.-W. Ham, S.B. Hong, *Appl. Catal. B* 53 (2004) 117–126.
- [25] L. Xiong, Q. Zhong, Q. Chen, S. Zhang, *Korean J. Chem. Eng.* 30 (2013) 836–841.
- [26] I. Mejía-Centeno, S. Castillo, R. Camposeco, J. Marín, L.A. García, G.A. Fuentes, *Chem. Eng. J.* 264 (2015) 873–885.
- [27] R. Camposeco, S. Castillo, V. Mugica, I. Mejía-Centeno, J. Marín, *Chem. Eng. J.* 242 (2014) 313–320.
- [28] S.G. Lee, H.J. Lee, I. Song, S. Youn, H. Kim do, S.J. Cho, *Sci. Rep.* 5 (2015) 12702.
- [29] G.T. Went, L.-J. Leu, R.R. Rosin, A.T. Bell, *J. Catal.* 134 (1992) 492–505.
- [30] G.T. Went, L.-J. Leu, A.T. Bell, *J. Catal.* 134 (1992) 479–491.
- [31] J.M. Cho, M.H. Sun, T.H. Kim, S.J. Cho, *J. Nanosci. Nanotechnol.* 10 (2010) 3336–3340.
- [32] I. Song, S. Youn, H. Lee, D.H. Kim, *Korean J. Chem. Eng.* 33 (2016) 2547–2554.
- [33] X. Chen, S.S. Mao, *Chem. Rev.* 107 (2007) 2891–2959.
- [34] S. Youn, S. Jeong, D.H. Kim, *Catal. Today* 232 (2014) 185–191.
- [35] A. Vandillen, R. Terorde, D. Lensveld, J. Geus, K. Debjong, *J. Catal.* 216 (2003) 257–264.
- [36] V.I.E. Bruyère, L.A. García Rodenas, P.J. Morando, M.A. Blesa, *J. Chem. Soc. Dalton Trans.* (2001) 3593–3597.
- [37] P. Malet, A. Muñoz-Páez, C. Martín, V. Rives, *J. Catal.* 134 (1992) 47–57.
- [38] S. Xiong, X. Xiao, Y. Liao, H. Dang, W. Shan, S. Yang, *Ind. Eng. Chem. Res.* 54 (2015) 11011–11023.
- [39] M. Yates, J.A. Martín, M.Á. Martín-Luengo, S. Suárez, J. Blanco, *Catal. Today* 107–108 (2005) 120–125.
- [40] N.-Y. Topsoe, T. Slabik, B.S. Clausen, T.Z. Srnak, J.A. Dumesic, *J. Catal.* 134 (1992) 742–746.
- [41] G. Madia, M. Koebel, M. Elsener, A. Wokaun, *Ind. Eng. Chem. Res.* 41 (2002) 4008–4015.
- [42] G. Bond, *Appl. Catal. A* 157 (1997) 91–103.
- [43] M.A. Centeno, J.J. Benítez, P. Malet, I. Carrizosa, J.A. Odriozola, *Appl. Spectrosc.* 51 (1997) 416–422.
- [44] D.A. Bulushev, L. Kiwi-Minsker, F. Rainone, A. Renken, *J. Catal.* 205 (2002) 115–122.
- [45] I. Giakoumelou, C. Fountzoula, C. Kordulis, S. Boghosian, *J. Catal.* 239 (2006) 1–12.
- [46] J. Li, G. Lu, G. Wu, D. Mao, Y. Guo, Y. Wang, Y. Guo, *Catal. Sci. Technol.* 4 (2014) 1268.
- [47] V. Syneček, F. Hanic, *Cechoslovackij fiziceskij zurnal* 4 (1954) 120–129.
- [48] T. Srnak, J. Dumesic, B. Clausen, E. Törnqvist, N.-Y. Topsøe, *J. Catal.* 135 (1992) 246–262.
- [49] M. Centeno, I. Carrizosa, J. Odriozola, *Appl. Catal. B* 19 (1998) 67–73.
- [50] C.-H. Lin, H. Bai, *Appl. Catal. B* 42 (2003) 279–287.
- [51] F. Hatayama, T. Ohno, T. Maruoka, T. Ono, H. Miyata, *J. Chem. Soc. Faraday Trans.* 87 (1991) 2629–2633.
- [52] N. Topsøe, J. Dumesic, H. Topsøe, *J. Catal.* 151 (1995) 241–252.
- [53] D.W. Kwon, K.H. Park, S.C. Hong, *Appl. Catal. A* 499 (2015) 1–12.
- [54] P.G.W.A. Kompiò, A. Brückner, F. Hippler, G. Auer, E. Löffler, W. Grünert, *J. Catal.* 286 (2012) 237–247.
- [55] L. Scatena, M. Brown, G. Richmond, *Science* 292 (2001) 908–912.
- [56] S.S.R. Putluru, L. Schill, A. Godiksen, R. Poreddy, S. Mossin, A.D. Jensen, R. Fehrmann, *Appl. Catal. B* 183 (2016) 282–290.
- [57] E. Broclawik, A. Góra, M. Najbar, *J. Mol. Catal. A: Chem.* 166 (2001) 31–38.
- [58] J.P. Chen, R.T. Yang, *Appl. Catal. A* 80 (1992) 135–148.
- [59] L. Lietti, G. Ramis, F. Berti, G. Toledo, D. Robba, G. Busca, P. Forzatti, *Catal. Today* 42 (1998) 101–116.
- [60] J.W. Choung, I.-S. Nam, S.-W. Ham, *Catal. Today* 111 (2006) 242–247.